HHS Public Access

Author manuscript

NMR Biomed. Author manuscript; available in PMC 2019 March 01.

Published in final edited form as:

NMR Biomed. 2018 March ; 31(3): . doi:10.1002/nbm.3864.

Investigation of the BOLD and CBV fMRI responses to somatosensory stimulation in awake marmosets (*Callithrix jacchus*)

Yoshiyuki Hirano[1,2], **Cecil C. Yen**[1], **Junjie V. Liu**[1], **Julie B. Mackel**[1], **Hellmut Merkle**[1], **George C. Nascimento**[1,3], **Bojana Stefanovic**[1,4], and **Afonso C. Silva**[1,*]

[1]Cerebral Microcirculation Section, Laboratory of Functional and Molecular Imaging, National Institute of Neurological Disorders and Stroke, National Institutes of Health, Bethesda, MD 20892-1065 USA

Abstract

Understanding the spatiotemporal features of the hemodynamic response function (HRF) to brain stimulation is essential to the proper application of neuroimaging methods to study brain function. Here, we investigated the spatiotemporal evolution of the blood oxygenation level-dependent (BOLD) and cerebral blood volume (CBV) HRF in conscious, awake marmosets (*Callithrix jacchus*), a New World nonhuman primate with a lissencephalic brain and with growing use in biomedical research. The marmosets were acclimated to head fixation and placed in a 7T MRI. Somatosensory stimulation (333 μs pulses, 2 mA amplitude, 64 Hz) was delivered bilaterally via pairs of contact electrodes. A block design paradigm was used in which the stimulus duration increased in pseudo-random order from a single pulse up to 256 electrical pulses (4 s). For CBV measurements, 30 mg/kg of iron oxide nanoparticles (MION) injected intravenously was used. Robust BOLD and CBV HRFs were obtained in S1, S2, and caudate at all stimuli conditions. In particular, BOLD and CBV responses to a single 333-μs-long stimulus were reliably measured, and the CBV HRF presented shorter onset time and time-to-peak than the BOLD HRF. Both the size of the regions of activation and the peak amplitude of the HRFs grew quickly with increasing stimulus duration, and saturated for stimulus durations greater than 1s. Onset times in S1 and S2 were faster than in caudate. Finally, the fine spatiotemporal features of the HRF in awake marmosets were similar to those obtained in humans, indicating that the continued refinement of awake non-human primate models is essential to maximize the applicability of animal fMRI studies to the investigation of human brain function.

Graphical Abstract

[*]Corresponding Author: Afonso C. Silva, Ph.D., Chief, Cerebral Microcirculation Section, Laboratory of Functional and Molecular Imaging, National Institute of Neurological Disorders and Stroke, National Institutes of Health, 49 Convent Drive MSC 1065 Building 49 Room 3A72, Bethesda MD 20892-1065 USA, Tel: (301)402-9703 Fax: (301) 480-2558, SilvaA@ninds.nih.gov.

[2]Present address: Research Center for Child Mental Development, Chiba University, 1-8-1 Inohana, Chuo-ku, Chiba 260-8670 JAPAN

[3]Present address: Departamento de Engenharia Biomédica, Universidade Federal do Rio Grande do Norte, Natal, RN 59075-000 Brazil

[4]Present address: Imaging Research, Sunnybrook Health Sciences Centre, 2075 Bayview Avenue Rm S6 50, Toronto, ON M4N 3M5 Canada

We investigated the spatiotemporal evolution of the BOLD and CBV fMRI responses to bilateral wrist stimulation of varying durations in conscious, awake marmosets. BOLD and CBV responses to a single 333-μs-long stimulus were reliably measured, and the CBV HRF presented a shorter onset time and time-to-peak. Both the size of the regions of activation and the peak amplitude of the HRFs grew quickly with stimulus duration, and saturated for stimulus durations greater than 1s.

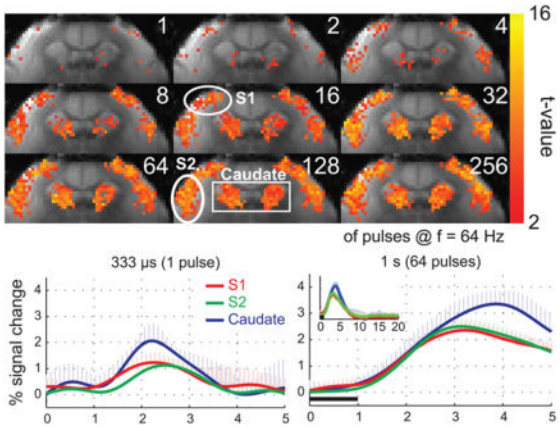

Keywords

BOLD; cerebral blood volume; functional neuroimaging; neurovascular coupling; non-human primate; somatosensory cortex

Introduction

The spatiotemporal characteristics of the hemodynamic response function (HRF) to focal changes in neural activity limit the resolution of functional neuroimaging techniques such as BOLD fMRI. In typical fMRI experiments, the stimulus is presented according to a block design paradigm in which periods of rest and stimulation are alternated. The HRF is obtained by statistical correlation of the fMRI time course with the stimulation paradigm [1,2]. Because the cerebral vasculature is a continuous, yet distributed network [3], the stimulus duration strongly influences the spatiotemporal characteristics of the HRF. Brief stimuli elicit vascular responses that consist mainly of dilatation of local capillaries and arterioles [4,5], which leads to local increases in cerebral blood volume (CBV) and flow (CBF), and an inflow of oxyhemoglobin and concomitant displacement of deoxyhemoglobin in the venules and veins, causing a BOLD effect [6]. Longer stimuli, on the other hand, recruit feeding arteries and draining veins that can be remotely located from the site of neural activity [7]. Proper understanding of the influence of the stimulus duration on the spatiotemporal features of the HRF is essential to both designs of functional neuroimaging experiments and interpretation of data.

Previously we investigated the spatiotemporal evolution of the HRF to ultra-short forelimb stimulation in chloralose-anesthetized rats [8]. We were able to determine that the HRF to a single 333-μs-long stimulus consisted of a rapid CBV and CBF response with an onset time

(OT) of 350 ms and a full width at half-maximum (FWHM) of 1 s, while longer stimuli elicited a dispersive transit of oxygenated blood across the cortical microvasculature that significantly prolonged the evolution of the CBV and the BOLD HRF [8]. We also observed a rapid growth of the spatial extent of activation with stimulus elongation, which demonstrated that functional hyperemia is an integrative process that involves the entire functional cortical depth.

In the present work, we investigate the spatiotemporal evolution of the BOLD and CBV HRF to somatosensory stimulation in conscious awake marmosets (*Callithrix jacchus*), a New World non-human primate with a brain size equivalent to the relative brain size of humans and approximately five times larger than the rat brain. Using stimulus parameters optimized in a previous publication [9], we obtained robust and reproducible fMRI responses in primary and secondary somatosensory cortex, as well as in the caudate. We show here that the BOLD and the CBV response to a single 333-μs-long stimulus can be robustly measured, and that the CBV HRF onsets and peaks significantly faster than the BOLD HRF. Both the size of the regions of activation and the peak amplitude of the BOLD HRFs grew quickly with increasing stimulus duration, and saturated for stimulus durations greater than 1s. The onset time of the BOLD HRF in S1 and S2 were faster than in caudate, which is consistent with some degree of serial processing between S1 and S2, and as expected, with thalamo-cortical processing preceding cortico-striatal processing. Finally, the fine spatiotemporal features of the HRF in awake marmosets are more similar to those of humans, indicating that the continued refinement of unanesthetized non-human primate models is essential to maximize the applicability of animal fMRI studies to the investigation of human brain function and to increase our understanding of the mechanisms of neurovascular coupling.

Materials and Methodology

Animal preparation

All experiments were approved by the NINDS/NIDCD Animal Care and Use Committee. Five adult male common marmosets (*Callithrix jacchus*, aged 7 – 8 years, body weight 260 – 400 g) from the NINDS colony were used. The marmosets were housed one or two to a cage with a twelve-hour light/dark cycle on an *ad libitum* diet of Purina New World primate biscuits, Zupreem canned marmoset food, water, PRANG oral rehydrator (Bio-Serv, Flemington, NJ), and fruit and vegetable treats. Prior to their use in the fMRI experiments, the marmosets were trained and acclimated to tolerate the rigid head restraint required to allow the acquisition of good quality data with acceptable levels of motion artifacts [10]. A progressive training schedule was devised to achieve full acclimation in three weeks, briefly described here:

Week 1 - acclimatization to body containment—Figure 1 shows the restraint setup used to train the awake marmosets. After being caught from its cage and transported to our lab, each marmoset was dressed with a sleeveless jacket (Lomir Biomedical, Inc. Malone, NY), which was closed by a longitudinal Velcro strip on the back. The jacket was attached to a plastic semi-cylindrical cover using plastic cable ties, and the marmoset was gently placed into the MRI cradle. The plastic body cover was secured to the cradle by nylon thumb

screws fastened to the sidebars on the cradle. The jacket prevented the marmosets from sliding out of the cradle. However, the animals could move their arms, legs, head and tail unimpededly, and were allowed to stretch and adjust their body position as needed for comfort. In the first week of training, the cradle was inserted into a mock MRI tube and the marmoset was observed from a distance via a webcam. Daily training sessions consisted of increasingly longer observation periods, starting with 15 minutes on day 1, and ending with one hour by day 4. Positive reinforcement in the form of 3–6 cc of vanilla-flavored nutritional supplement (Pediasure, Abbott Labs, Abbott Park, IL) and 3–5 mini-marshmallows were given at the beginning and end of each training session.

Week 2 - acclimatization to body containment in the presence of MRI sounds —Because MRI is a loud technique, it is necessary to acclimatize the animals to the sounds generated by the MRI scanner during imaging. In week 2, the animals were restrained as in week 1 for increasing periods of time, during which the sounds produced by the MRI scanner were played out at a softer level than in a real MRI session. This schedule reinforced the adaptation to the body restraint initiated in week 1, and conditioned the animals to ignore the MRI sounds produced by the scanner. Pediasure and mini-marshmallows were used as positive reinforcements at the beginning and at the end of each training session.

Week 3 - acclimatization to head restraint in the presence of MRI sounds— Traditionally, the use of awake, conscious animals in the MRI requires the surgical implantation of head posts that can be rigidly secured by clamps to a specially designed frame [11]. Three of the five marmosets included in the present study were equipped with head-posts. The week following completion of the second week of training, a head implant consisting of two low-profile round bases made of PEEK plastic and treaded on the inside were surgically attached to the anterior and the posterior bases of the skull using dental acrylic cement (Lang Dental Manufacturing Co, Wheeling, IL) and nylon screws (size 0–80, 2.4 mm long, Plastics One, Roanoke, VA). The animals were allowed 2 weeks to recover from surgery prior to engaging in the third and final week of acclimatization. For restraining their heads, two ¼″ round solid peek rods, 50 mm in length, were treaded onto the round bases and clamped to a home-built frame. While the use of head posts allows maximum restraint of the animals, it brings in many disadvantages. Amongst them, susceptibility artifacts that degraded image quality by introducing geometric distortions and/or signal dropouts in the MR images, and the constant need to perform aseptic cleaning to prevent infections, made us think of an alternative to the use of head implants by designing custom-fit helmets to match the contour of each individual head exactly, providing a comfortable, yet effective restraint (Fig. 1). To design the helmet pieces, a 3D gradient-echo MRI of the entire head and neck was acquired from each of the remaining two subjects in this study. Next, a contour of the head was obtained by a 3D surface rendering algorithm and fed into “Rhinoceros 3D” (McNeel North America, Seattle, WA), a 3D modeling program, to design the top (head) and bottom (chin) helmet pieces, which were manufactured from liquid ABS plastic using a 3D printer (ProJet HD3000, 3D Systems Corp., Rock Hill, SC). To provide greater comfort for the animals, the inside surface of both top and bottom pieces were lined up with 3 mm thick foam. The marmosets were then restrained to the bed by the body cover, as in the previous weeks, and then fitted with their custom-built helmets, as shown in Fig. 1.

In week 3, the animals were conditioned for increasing periods of time, as in the first two weeks. While in the mock MRI tube, they were allowed to hear the sounds produced by the MRI scanner, played out at the same level of loudness as in a real MRI session. This schedule reinforced the adaptation to the body restraint of the previous weeks, and further conditioned the animals to ignore the MRI sounds produced by the scanner, while enforcing full head fixation. At the end of the third week of training, all five animals successfully completed the acclimatization procedure (see Results).

Following the acclimatization training, the marmosets were taken to the MRI scanner for functional experiments. The animals were dressed with the sleeveless jacket and secured in the sphinx position to the MRI cradle. Their heads were fixed with head posts (3 individuals) or with the two-piece helmet restraint (other 2 individuals). For the actual fMRI scans, earplugs made of silicon jelly (Insta-Putty, Insta-Mold Products, Inc., Oaks, PA) were carefully pressed into the ear canals and covered with acoustical foam pads from both sides of the head. This further restrained head motion and protected the animals from the much louder MRI scanner noise. The tail was shaved and an indwelling intravenous catheter was placed into the lateral tail vein for administration of MR contrast agents. Prior to being pushed into the MRI bore, the animals were fed with Pediasure ad libitum. Once inside the MRI, the animals were continuously monitored via an MRI-compatible camera (MRC Systems GmbH, Heidelberg, Germany) connected to a personal computer (PC) placed by the operator’s desk.

MRI Methods

fMRI experiments were performed in a horizontal 7T/30 cm magnet (Bruker-Biospin, Billerica, MA, USA) equipped with a 15 cm gradients capable of 450 mT/m amplitude within 120 μs rise-time (Resonance Research Inc., Billerica, MA, USA). A home-built two-element receive-only surface coil array (1.6 cm ID) was positioned over the head implants or outside the helmets near somatosensory cortex, and connected to home-built preamplifiers. BOLD-fMRI data was obtained with a gradient-recalled echo (GRE) echo-planar-imaging (EPI) sequence in a single coronal slice with the following parameters: In experiment 1, field-of-view (FOV) = 32.4 × 32.4 mm^2, matrix = 108 × 108, slice thickness = 2 mm, nominal resolution = 300 × 300 × 2000 μm^3, acquisition bandwidth = 333 kHz, TE = 20 ms, TR = 250 ms, Flip angle = 30°. In experiments 2 and 3, FOV = 25.6 × 25.6 mm^2, matrix = 64 × 64, slice thickness = 2 mm, nominal resolution = 400 × 400 × 2000 μm^3, acquisition bandwidth = 200 kHz, TE = 13–15 ms, TR = 250 ms. After the fMRI sessions, an anatomical image was acquired with same FOV as in the fMRI acquisition using a RARE sequence (TE = 15 ms, TR = 3 s, Flip angle = 90°, Matrix = 240 × 216, RARE factor = 8, Number of average = 4).

Somatosensory Stimulation

To measure the HRF to somatosensory stimulation, a pair of contact electrodes was secured across each wrist and bilateral electrical stimulation (333 μs pulses, 2 mA amplitude, 64 Hz) was performed synchronized with the scanner and controlled from a PC running Presentation (Neurobehavioral Systems, Inc., Albany, CA, USA). Three experiments were performed. In Experiment 1, the BOLD HRFs to stimuli of different durations were

measured. A block-design paradigm was run containing trials of 9 × 30 s-long off-on-off epochs in which the stimulus consisted of 1, 2, 4, 8, 16, 32, 64, 128 or 256 electrical pulses (333 μs – 4 s stimulus duration). The 4.5 min-long trials were repeated in randomized order 16 times. In addition, the BOLD impulse response function (IRF) was measured during presentation of 128 trials of a single 30 s-long off-on-off epoch containing a single electrical pulse (333 μs stimulus duration). In Experiment 2, the dose of ultrasmall superparamagnetic iron oxide (USPIO) contrast agent for CBV measurements was optimized. An initial dose of 20 mg/kg of 30 nm (USPIO) particles (Molday ION, Biophysics Assay Laboratory, Inc., Worcester, MA) was injected to the animals intravenously. Five minutes were allowed for equilibration of the USPIO concentration in blood prior to starting the CBV measurements. The trial, consisting of a single 30-s long off-on-off epoch of fixed stimulus duration (256 electrical pulses = 4 s), was repeated 16 times. At the end of the measurement, an additional injection of 10mg/kg USPIO to take the total dose to 30 mg/kg was given and another 5 min allowed prior to repeating the CBV measurements. Finally, in experiment 3, the CBV-IRF was measured during presentation of 128 trials of a single 30 s-long off-on-off epoch containing a single electrical pulse (333 μs stimulus duration).

Data Analysis

Data preprocessing consisted of in-plane motion correction using SPM5 (Wellcome Department of Imaging Neuroscience, University College London, London, UK). Baseline drift was removed and the series of 120 images (30 s) corresponding to each stimulus duration were identified and averaged across the epochs. High-frequency noise components were removed by filtering the averaged time courses with a 1 Hz square filter apodized with a 1.5 Hz Hanning window. After data preprocessing, region of interest (ROI) analysis was performed. A functional t-map mask was generated by identifying regions of activation to the 4 s stimulus task ($P < 0.05$). Then, the position of the primary (S1) and secondary (S2) somatosensory cortices, and caudate were identified for each subject, and the location of the ROIs were further refined by multiplying the functional mask with a mask obtained from the anatomical image. For each subject, the number of activated voxels, maximum percent signal change, time-to-peak (TTP) and onset time (OT) were computed following a 16-fold Fourier interpolation and normalization to the mean of the pre-stimulus period. OT was defined as the time to 10 % of peak after fitting a three gamma function[12]. One-way analysis of variance (ANOVA), followed by Scheffe post hoc test, was performed to determine statistical significance of differences in TTP and OT, respectively.

Results

Acclimatization to head restraint

To obtain a measure of their tolerance to the acclimatization procedures, the marmosets were evaluated and scored according to the Behavioral Assessment Scale [13] listed on Table 1 prior to, during and after each of the 3 acclimatization weeks. All five subjects acclimatized well to being restrained in the MRI-compatible bed. In week 1, the marmosets started with an average score of 2.0 ± 0.0 on the Behavioral Assessment Scale and acclimatized to an average score of 1.0 ± 0.0 by the end of the week. In week 2, the average score started at 1.0 ± 0.0 and ended at 1.5 ± 0.7 due to the introduction of the MRI sounds and the prolonged

restraint period. Finally, in week 3, with the introduction of the head restraint, the initial score was 2.5 ± 0.7 on day 1 and improved to 1.5 ± 0.7 at the end of the training. We also evaluated the Behavioral Assessment Score on the first day in the MRI scanner, and all animals obtained a score of 1.0.

All MRI sessions lasted less than four hours, during which all subjects were monitored through an in-bore camera. No agitation due to the MRI noise or to the functional stimulations was noted in any of the marmosets.

BOLD HRF to different stimuli durations

Figure 2 shows the BOLD activation maps from a representative individual marmoset in response to stimuli of different durations. Areas of activation in S1 and S2 grew from just a few voxels located in the middle and upper layers of the respective regions in response to a single pulse stimulus, to occupy the entire cortical regions with longer stimulus durations of up to sixty-four pulses (1 s), beyond which no additional expansion was observed. In caudate, the response grew even more rapidly, so that by thirty-two pulses (0.5 s), the entire area was active and no further expansion was observed (Fig. 2).

Figure 3 shows the mean BOLD HRFs to stimuli of different durations, averaged within the three ROIs (S1, S2, and caudate) and then across all five subjects. Robust BOLD HRFs were obtained in all 3 ROIs for all stimulus durations. The caudate region presented the strongest BOLD response, while S1 and S2 presented equivalent peak amplitudes. The amplitude of the BOLD HRF grew from 1.3 ± 0.4, 1.2 ± 0.2 and 2.2 ± 0.5 % in S1, S2 and caudate, respectively, in response to a single pulse, to 2.4 ± 0.3, 2.5 ± 0.3 and 3.4 ± 0.5%, respectively, in response to 64 pulses (1s). Longer stimulus durations produced no additional increases in the peak amplitude of the BOLD HRF (Table 2). This saturation in the peak amplitude of the BOLD HRF can also be appreciated in the bottom 3 panels of Fig. 3.

Figure 4 summarizes the mean growth in the number of active voxels (Fig. 4A), peak BOLD amplitude (Fig. 4B) and TTP (Fig. 4C) with stimulus duration in S1, S2, and caudate, averaged across all five subjects. All 3 regions presented a monotonic increase of the number of active voxels and peak amplitude with stimulus durations up to 1s, and saturation of both measures for longer stimuli. Interestingly, the caudate region presented the lowest number of active voxels, but the highest BOLD amplitude at all stimulus durations, and also the longest TTPs. Figure 4D shows the mean OT for each of the 3 regions, averaged across subjects. The OT in S1 (1.0 ± 0.3 s), was significantly shorter than that in S2 (1.2 ± 0.2 s) and caudate (1.2 ± 0.3 s) (one-way ANOVA followed by Scheffe post hoc test, $F(2,178) = 12.72$, $P < 0.001$), suggesting a hierarchy of activation between the 3 regions.

Optimization of the dose of USPIO for CBV measurements

To examine effective dose of USPIO for CBV measurements, the CBV HRF to a 4 s stimulus was evaluated at two different doses, 20 mg/kg and 30 mg/kg. Figure 5A shows the BOLD and the CBV t-score maps in a representative marmoset. Robust activations in S1, S2 and caudate were obtained with BOLD contrast. However, there was no clearly detectable CBV activation in caudate at either of the two tested USPIO dosages. This was consistently observed across all five subjects. The size of the CBV regions of activation in S1 and S2

decreased at the larger USPIO dose with respect to the smaller dose, presumably due to the higher T_2^* dephasing achieved at the higher dose that lowered the baseline SNR of the images. Fig. 5B shows the mean BOLD HRF (top graph) and the mean CBV HRFs obtained with the lower dose (middle graph) and the higher dose of USPIO (bottom graph), in response to a 4 s stimulus, averaged across all five subjects. Compared to the peak amplitude of the CBV HRF obtained with the lower dose, the maximum relative percent signal change obtained with the higher dose was 32 % and 34 % larger, respectively. For this reason, and to avoid BOLD contributions to the CBV measurements [14], we adopted 30 mg/kg USPIO as the more appropriate dose for carrying out the investigation of the CBV impulse response function.

BOLD and CBV impulse response function

Figure 6 shows the mean BOLD- and CBV-IRFs averaged across the five marmosets. To allow comparison of their temporal characteristics with the BOLD-IRFs, the sign of the CBV time-courses were flipped. Figure 6A shows the BOLD- and CBV-IRF measured in S1, while Fig. 6B shows the time-courses measured in S2. Compared to the BOLD-IRF, the CBV-IRF showed a quick onset in response to the brief stimulus, and a shorter TTP as well. The CBV onset times in S1 (0.5 ± 0.2 s) and in S2 (0.7 ± 0.2 s) were significantly shorter than the respective BOLD onset times (1.1 ± 0.3 s in S1 and 1.3 ± 0.4 s in S2, $P < 0.001$, Fig. 6C). The CBV TTPs were 2.2 ± 0.6 s in S1 and 2.2 ± 0.2 s in S2, significantly shorter than the respective BOLD TTPs (2.7 ± 0.2 s in S1 and 3.0 ± 0.1 s in S2, $P < 0.001$, Fig. 6D).

Discussion

In the present work, we investigated the BOLD and the CBV functional responses to short somatosensory stimulation in conscious, awake marmosets. We developed a simple yet effective acclimatization protocol to condition and trained the marmosets to tolerate physical restraint during the data acquisition, and we designed a helmet-based head restraint that is completely non-invasive and able to hold the head still without sacrificing comfort. After undergoing such training, the marmosets produced robust and reproducible fMRI responses in S1, S2, and caudate, in full agreement with our previous publication [9]. We were able to reliably detect the BOLD and the CBV response to a single 333-μs-long stimulus. We observed that the CBV HRF onsets and peaks significantly faster than the BOLD HRF, indicating a significant arterial contribution to the CBV response. By varying the stimulus duration, we observed a quick growth and saturation of both the size of the regions of activation and the peak amplitude of the BOLD HRFs for stimulus durations greater than 1s. The onset times of the BOLD HRF in S1 and S2 were faster than in caudate, which is consistent with some degree of serial processing between S1 and S2, and as expected, with thalamo-cortical processing preceding cortico-striatal processing.

Acclimatization procedures

Because animals are inherently noncompliant, most MRI experiments performed to date on animal models have required the use of anesthesia. While being second to none in alleviating stress, anesthesia brings in a number of drawbacks. Anesthesia has a profound effect on the autonomous nervous system, requiring monitoring and control the systemic physiological

status of the animal. Furthermore, anesthesia produces long-lasting effects on the animal physiology that may influence longitudinal studies [15]. Anesthesia also interferes with neural activity [16] and vascular tone [17], therefore affecting neurovascular coupling in not well understood ways [18] and compromising the interpretability and applicability of fMRI data to the understanding of normal brain function. In a recent publication, we compared the BOLD fMRI response to somatosensory stimulation in awake versus propofol-anesthetized marmosets [9]. We found that the responses in S1, S2 and caudate were significantly stronger in awake animals, while anesthesia completely abolished response in caudate. Moreover, anesthesia influenced the shape of the HRF and S1–S2 spontaneous functional connectivity [9]. Thus, the ability to acquire physiological responses in conscious, awake animal models represents a necessary step towards better investigating brain.

One approach to enforcing compliance that eliminates the need for anesthesia involves training the animal to tolerate physical restraint during data acquisition. The three-week acclimatization protocol developed in our lab [10] proved simple and effective in conditioning and training the marmosets to tolerate long periods of restraint with minimal levels of stress. Stress can introduce significant confounds in studies of brain function, and thus it is important to research and develop effective training protocols for imaging awake animals [19]. The use of individualized, anatomically exact helmets played a large role in ensuring comfortable head restraint. The use of helmets is significantly advantageous over the more traditional head-fixation method of surgically implanted head posts. Head implants are typically associated with lower data quality due to susceptibility artifacts in the form geometric distortions and/or signal dropouts introduced by the dental cement and fixation screws. In addition, head implants degrade with time and require regular aseptic cleaning to prevent infections. More, if the animal needs to be treated with antibiotics and/or anti-inflammatory drugs for an eventual infection, the treatment may interfere with neurovascular coupling, thus compromising interpretation of the data. Moreover, much of the major advantage of MRI as a non-invasive technique is lost with the use of head implants. The use of helmets as a non-invasive restraint device allows the use of the animal in indefinitely prolonged longitudinal studies. The helmets also permit better placement of receive-only RF coils closer to the skull of the animal, a key factor for improved SNR. In fact, we have recently embedded low profile RF coil arrays inside the helmets to further improve SNR [20].

Spatiotemporal characteristics of BOLD HRF to brief stimulation

Robust BOLD HRFs were obtained in S1, S2, and caudate, even when the stimulus consisted of a single 333 μs long pulse. In S1 and S2, activation began in the central layers of the cortex, and grew quickly to occupy all layers by 64 pulses (1 s) stimulus duration. This fast spatial filling of the entire cortical depth is consistent with our previous data obtained from α-chloralose anesthetized rats [8] and our follow-up study in awake marmosets[21], showing that functional hyperemia is an integrative process that involves the entire functional cortical depth. As well in caudate, there was an equally fast growth in the area of activation, with most of the caudate area of activation filled in response to a 1 s long stimulus. The onset time of the BOLD HRF in S1 was shorter than that of S2 and caudate. The shorter onset in S1 is in agreement with previous MEG studies in humans [22,23], and consistent with serial processing between S1 and S2 [24], but cannot refute the possibility of

parallel processing as well [25,26]. Of the 3 areas, caudate had the longest onset time, suggesting activation of caudate happens via cortico-striatal projections [27] that are preceded by the thalamo-cortical projections into S1 and S2.

We observed saturation of both the peak amplitude and TTP of the BOLD HRF in all three regions for stimuli longer than 128 pulses (2 s). This saturation of the peak BOLD amplitude implies that a linear relationship between the BOLD response and the neural activity [28–30], in which both the amplitude and the area under the BOLD response increase linearly with stimulus duration, can be supported for stimulus durations up to 64 pulses (1 s). For stimulus durations longer than 128 pulses (2 s), the BOLD peak amplitude becomes constant, whereas the area under the curve and FHWM increase linearly with stimulus duration [29].

The location and size of the areas of activation in S1 and S2 agree well with previous histological and electrophysiological studies in marmosets mapping area 3b, the main homolog area of S1 of other mammals [31], and area S2, respectively [32,33]. Area 3b extends 2 mm in the rostrocaudal direction, and spans 8 mm lateral to the midline before bending rostrally and extending 6 mm further [32]. The hand representation is located immediately medial to this bend, and spans 2 mm in the mediolateral direction [33]. Thus, considering that the cortical thickness in marmosets is approximately 2 mm, the hand representation within area 3b in each hemisphere spans about 8 mm^3, or 45 voxels, in agreement with the total number of activated voxels shown in Fig. 4A. On the other hand, S2 is located on the upper bank of the lateral sulcus immediately adjoining the caudolateral portion of S1 that represents the upper lip, and the hand and the arm are represented in the more medial parts of S2 [33]. Interestingly, the number of activated voxels in S2 was nearly double that of S1 (Fig. 4A). Reasons for the larger regions of activation in S2 are not entirely clear, but could be related to the fact that the receptive fields of different areas of the body, including the hands and the arms, are much larger in S2 than in S1 [33]. Further studies are needed to fully investigate this issue.

The caudate is an area known to receive inputs both from motor and somatosensory cortices as well as from thalamus [34,35]. In our previous publication comparing BOLD fMRI response in awake marmosets to those obtained in animals anesthetized with propofol, the caudate also produced robust and reproducible responses under awake conditions, but not under anesthesia [9]. Interestingly, the fMRI response in caudate obtained here was stronger than in the previous publication, and stronger than the responses in S1 and S2. A possible explanation is that the present study employed bilateral stimulation and a thicker slice (2 mm) compared to the previous work. These experimental differences may have contributed to a better integration of functional activity in the caudate.

Comparison of temporal characteristics between BOLD and CBV

Robust BOLD and CBV responses to a single 333 μs pulse were obtained. In S1, the CBV HRF consists of a short OT = 0.5 s and TTP = 2.2 s, both parameters significantly shorter than those of the BOLD HRF (OT = 1.3 s; TTP = 2.7 s). In S2 the respective parameters were longer than in S1, again consistent with some degree of serial processing between S1 and S2. We interpret the temporal lag of the BOLD HRF to be due to influence of the arteriole–venule transit time [8,36,37]. For short stimuli (< 1s), the local hemodynamic changes

involve an active redistribution of blood flow and volume within the capillary network and cortical arterioles and venules [4,8,36]. We have previously demonstrated in anesthetized rats that the temporal evolution of the functional CBF and CBV responses to a short stimulus are well matched, because of the contained involvement of the local microvasculature and the small relative changes in CBF and CBV associated with the short stimulus [8]. In the present work, we were not able to implement ASL techniques to measure CBF. It will be interesting in the future to verify the temporal match of CBF and CBV responses in awake marmosets.

It is interesting to compare the temporal characteristics of the HRF in marmosets to data obtained in other species. The TTP of the CBV HRF (2.2 s) and BOLD HRF in S1 (2.7 s) were longer than the respective TTP obtained in α-chloralose anesthetized rats (CBV 1.1 s, BOLD 1.5 s) [8], but shorter than the TTP obtained in the human visual cortex (BOLD 4.51 s) [38], indicating that the cortical microvascular length in marmosets may be more similar to humans than to rodents, presenting an elongated dispersive contribution of the transit of deoxyhemoglobin through the post-capillary side of the cerebral vasculature. On the other hand, serial processing between S1 and S2 seen in the present study seems to disagree with the result from the anesthetized cats, which showed no differences in onset time between primary and secondary visual cortices [39]. This may be due to the fact that thalamus projects to both primary and secondary visual cortices in cat, unlike most primates that secondary sensory cortices receive input merely from primary cortices.

In conclusion, the present study demonstrated the feasibility of measuring both the BOLD and the CBV HRF to extremely brief stimuli in conscious, awake marmosets that were acclimated to head fixation. Robust and reproducible fMRI responses were obtained in S1, S2, and caudate, and the shorter onset times in S1 suggest the HRF starts in S1 and propagates in hierarchical order along the sensory pathway. Finally, the fine spatiotemporal features of the HRF in awake marmosets are more similar to those of humans, indicating that the continued refinement of unanesthetized non-human primate models is essential to maximize the applicability of animal fMRI studies to the investigation of human brain function and to increase our understanding of the mechanisms of neurovascular coupling.

Acknowledgments

The authors are deeply indebted to Dr. Alan P. Koretsky for enlightening scientific discussions, and to Mrs. Xian Feng (Lisa) Zhang for her invaluable help in animal preparation. This research was supported by the Intramural Research Program of the NIH, NINDS (Alan P. Koretsky, Scientific Director).

List of Abbreviations

ANOVA	analysis of variance
ASL	arterial spin labeling
BOLD	blood oxygen level dependent
CBF	cerebral blood flow
CBV	cerebral blood volume

EPI	echo planar imaging
fMRI	functional magnetic resonance imaging
FOV	field of view
FWHM	full width at half-maximum
GRE	gradient-recalled echo
HRF	hemodynamic response function
IRF	impulse response function
MION	monocrystalline iron oxide nanoparticles
OT	onset time
RARE	rapid acquisition with relaxation enhancement
ROI	region of interest
S1	primary somatosensory cortex
S2	secondary somatosensory cortex
TE	echo time
TR	repetition time
TTP	time to peak
USPIO	ultrasmall superparamagnetic iron oxide

References

1. Bandettini PA, Jesmanowicz A, Wong EC, Hyde JS. Processing strategies for time-course data sets in functional MRI of the human brain. Magnetic resonance in medicine : official journal of the Society of Magnetic Resonance in Medicine/Society of Magnetic Resonance in Medicine. 1993; 30(2):161–173.
2. Friston KJ, Holmes AP, Poline JB, et al. Analysis of fMRI time-series revisited. NeuroImage. 1995; 2(1):45–53. [PubMed: 9343589]
3. Duvernoy HM, Delon S, Vannson JL. Cortical blood vessels of the human brain. Brain research bulletin. 1981; 7(5):519–579. [PubMed: 7317796]
4. Stefanovic B, Hutchinson E, Yakovleva V, et al. Functional reactivity of cerebral capillaries. Journal of cerebral blood flow and metabolism : official journal of the International Society of Cerebral Blood Flow and Metabolism. 2008; 28(5):961–972.
5. Tian P, Teng IC, May LD, et al. Cortical depth-specific microvascular dilation underlies laminar differences in blood oxygenation level-dependent functional MRI signal. Proceedings of the National Academy of Sciences of the United States of America. 2010; 107(34):15246–15251. [PubMed: 20696904]
6. Ogawa S, Lee TM, Kay AR, Tank DW. Brain magnetic resonance imaging with contrast dependent on blood oxygenation. Proceedings of the National Academy of Sciences of the United States of America. 1990; 87(24):9868–9872. [PubMed: 2124706]
7. Turner R. How much cortex can a vein drain? Downstream dilution of activation-related cerebral blood oxygenation changes. Neuro Image. 2002; 16(4):1062–1067. [PubMed: 12202093]

8. Hirano Y, Stefanovic B, Silva AC. Spatiotemporal evolution of the functional magnetic resonance imaging response to ultrashort stimuli. The Journal of neuroscience : the official journal of the Society for Neuroscience. 2011; 31(4):1440–1447. [PubMed: 21273428]
9. Liu JV, Hirano Y, Nascimento GC, Stefanovic B, Leopold DA, Silva AC. fMRI in the awake marmoset: somatosensory-evoked responses, functional connectivity, and comparison with propofol anesthesia. Neuroimage. 2013; 78:186–195. [PubMed: 23571417]
10. Silva AC, Liu JV, Hirano Y, et al. Longitudinal functional magnetic resonance imaging in animal models. Methods Mol Biol. 2011; 711:281–302. [PubMed: 21279608]
11. Stefanacci L, Reber P, Costanza J, et al. fMRI of monkey visual cortex. Neuron. 1998; 20(6):1051–1057. [PubMed: 9655492]
12. Shan ZY, Wright MJ, Thompson PM, et al. Modeling of the hemodynamic responses in block design fMRI studies. J Cereb Blood Flow Metab. 2014; 34(2):316–324. [PubMed: 24252847]
13. Schultz-Darken NJ, Pape RM, Tannenbaum PL, Saltzman W, Abbott DH. Novel restraint system for neuroendocrine studies of socially living common marmoset monkeys. Lab Anim. 2004; 38(4): 393–405. [PubMed: 15479554]
14. Lu H, Scholl CA, Zuo Y, Stein EA, Yang Y. Quantifying the blood oxygenation level dependent effect in cerebral blood volume-weighted functional MRI at 9.4T. Magnetic resonance in medicine : official journal of the Society of Magnetic Resonance in Medicine/Society of Magnetic Resonance in Medicine. 2007; 58(3):616–621.
15. Wegener S, Wong EC. Longitudinal MRI studies in the isoflurane-anesthetized rat: long-term effects of a short hypoxic episode on regulation of cerebral blood flow as assessed by pulsed arterial spin labelling. NMR Biomed. 2008; 21(7):696–703. [PubMed: 18275045]
16. Franks NP. General anaesthesia: from molecular targets to neuronal pathways of sleep and arousal. Nat Rev Neurosci. 2008; 9(5):370–386. [PubMed: 18425091]
17. Matta BF, Heath KJ, Tipping K, Summors AC. Direct cerebral vasodilatory effects of sevoflurane and isoflurane. Anesthesiology. 1999; 91(3):677–680. [PubMed: 10485778]
18. Masamoto K, Fukuda M, Vazquez A, Kim SG. Dose-dependent effect of isoflurane on neurovascular coupling in rat cerebral cortex. Eur J Neurosci. 2009; 30(2):242–250. [PubMed: 19659924]
19. King JA, Garelick TS, Brevard ME, et al. Procedure for minimizing stress for fMRI studies in conscious rats. J Neurosci Methods. 2005; 148(2):154–160. [PubMed: 15964078]
20. Papoti D, Yen CC, Mackel JB, Merkle H, Silva AC. An embedded four-channel receive-only RF coil array for fMRI experiments of the somatosensory pathway in conscious awake marmosets. NMR Biomed. 2013; 26(11):1395–1402. [PubMed: 23696219]
21. Yen CC-C, Papoti D, Silva AC. Investigating the spatiotemporal characteristics of the deoxyhemoglobin-related and deoxyhemoglobin-unrelated functional hemodynamic response across cortical layers in awake marmosets. Neuro Image. 2017; doi: 10.1016/j.neuroimage.2017.03.005
22. Del Gratta C, Della Penna S, Ferretti A, et al. Topographic organization of the human primary and secondary somatosensory cortices: comparison of fMRI and MEG findings. Neuro Image. 2002; 17(3):1373–1383. [PubMed: 12414277]
23. Lin YY, Forss N. Functional characterization of human second somatosensory cortex by magnetoencephalography. Behavioural brain research. 2002; 135(1–2):141–145. [PubMed: 12356444]
24. Khoshnejad M, Piche M, Saleh S, Duncan G, Rainville P. Serial processing in primary and secondary somatosensory cortex: A DCM analysis of human fMRI data in response to innocuous and noxious electrical stimulation. Neuroscience letters. 2014; 577:83–88. [PubMed: 24933536]
25. Rowe MJ, Turman AB, Murray GM, Zhang HQ. Parallel organization of somatosensory cortical areas I and II for tactile processing. Clinical and experimental pharmacology & physiology. 1996; 23(10–11):931–938. [PubMed: 8911737]
26. Zhang HQ, Zachariah MK, Coleman GT, Rowe MJ. Hierarchical equivalence of somatosensory areas I and II for tactile processing in the cerebral cortex of the marmoset monkey. Journal of neurophysiology. 2001; 85(5):1823–1835. [PubMed: 11352999]

27. Wiesendanger E, Clarke S, Kraftsik R, Tardif E. Topography of cortico-striatal connections in man: anatomical evidence for parallel organization. Eur J Neurosci. 2004; 20(7):1915–1922. [PubMed: 15380013]
28. Boynton GM, Engel SA, Glover GH, Heeger DJ. Linear systems analysis of functional magnetic resonance imaging in human V1. The Journal of neuroscience : the official journal of the Society for Neuroscience. 1996; 16(13):4207–4221. [PubMed: 8753882]
29. Pfeuffer J, McCullough JC, Van de Moortele PF, Ugurbil K, Hu X. Spatial dependence of the nonlinear BOLD response at short stimulus duration. Neuro Image. 2003; 18(4):990–1000. [PubMed: 12725773]
30. Birn RM, Bandettini PA. The effect of stimulus duty cycle and “off” duration on BOLD response linearity. Neuro Image. 2005; 27(1):70–82. [PubMed: 15914032]
31. Kaas JH. What, if anything, is SI? Organization of first somatosensory area of cortex. Physiological reviews. 1983; 63(1):206–231. [PubMed: 6401864]
32. Burish MJ, Stepniewska I, Kaas JH. Microstimulation and architectonics of frontoparietal cortex in common marmosets (Callithrix jacchus). The Journal of comparative neurology. 2008; 507(2): 1151–1168. [PubMed: 18175349]
33. Krubitzer LA, Kaas JH. The organization and connections of somatosensory cortex in marmosets. The Journal of neuroscience : the official journal of the Society for Neuroscience. 1990; 10(3): 952–974. [PubMed: 2108231]
34. Villablanca JR. Why do we have a caudate nucleus? Acta neurobiologiae experimentalis. 2010; 70(1):95–105. [PubMed: 20407491]
35. Robinson JL, Laird AR, Glahn DC, et al. The functional connectivity of the human caudate: an application of meta-analytic connectivity modeling with behavioral filtering. Neuro Image. 2012; 60(1):117–129. [PubMed: 22197743]
36. Hutchinson EB, Stefanovic B, Koretsky AP, Silva AC. Spatial flow-volume dissociation of the cerebral microcirculatory response to mild hypercapnia. Neuro Image. 2006; 32(2):520–530. [PubMed: 16713717]
37. Silva AC, Koretsky AP, Duyn JH. Functional MRI impulse response for BOLD and CBV contrast in rat somatosensory cortex. Magnetic resonance in medicine : official journal of the Society of Magnetic Resonance in Medicine/Society of Magnetic Resonance in Medicine. 2007; 57(6):1110–1118.
38. de Zwart JA, Silva AC, van Gelderen P, et al. Temporal dynamics of the BOLD fMRI impulse response. Neuro Image. 2005; 24(3):667–677. [PubMed: 15652302]
39. Yen CC, Fukuda M, Kim SG. BOLD responses to different temporal frequency stimuli in the lateral geniculate nucleus and visual cortex: insights into the neural basis of fMRI. Neuro Image. 2011; 58(1):82–90. [PubMed: 21704712]

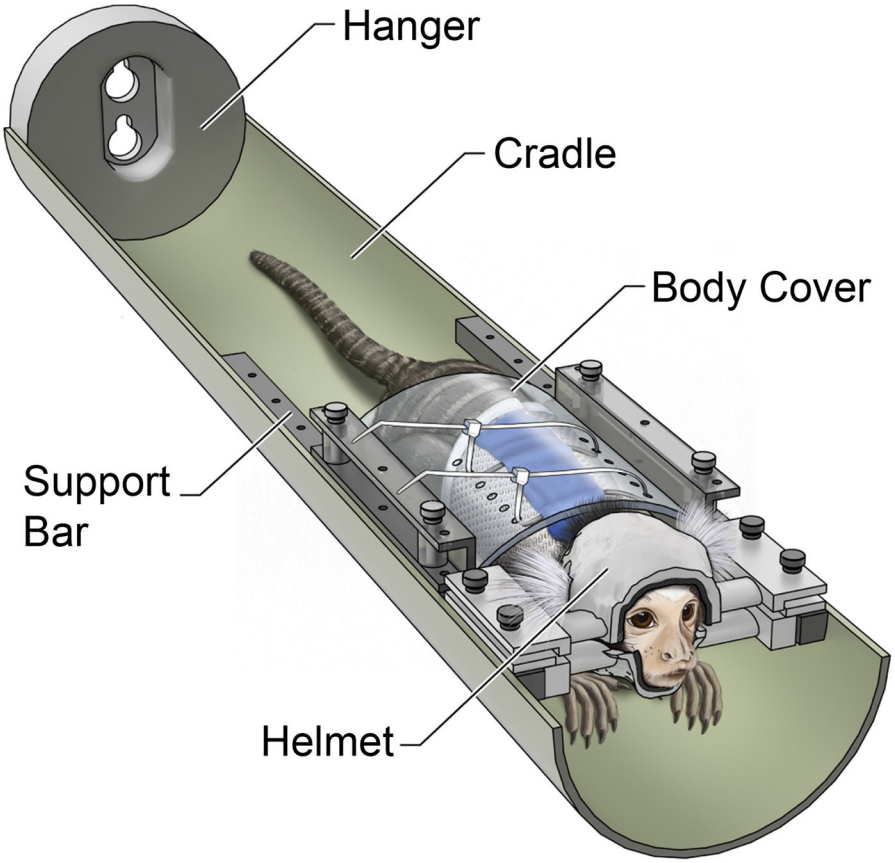

Figure 1.

(A) Illustration of the restraint setup used to train and to image marmosets. The animal wears a sleeveless jacket which is attached to a plastic back cover. The back cover is fastened to the sidebars on the cradle, preventing the animal from sliding out. At all times, the arms, legs, and tail of the animal are free to move. The head of the marmoset is secured by a two-piece, custom-built helmet made specifically for that individual. The chin piece on the bottom supports the chin of the animal, and the head piece on the top prevents head motion. Both helmet pieces are lined up with foam on the inside to provide a comfortable support to the entire head. The animal sits in the sphinx position looking out towards the back of the magnet. The bed is secured to the bed sliding mechanism on one end via the hanger.

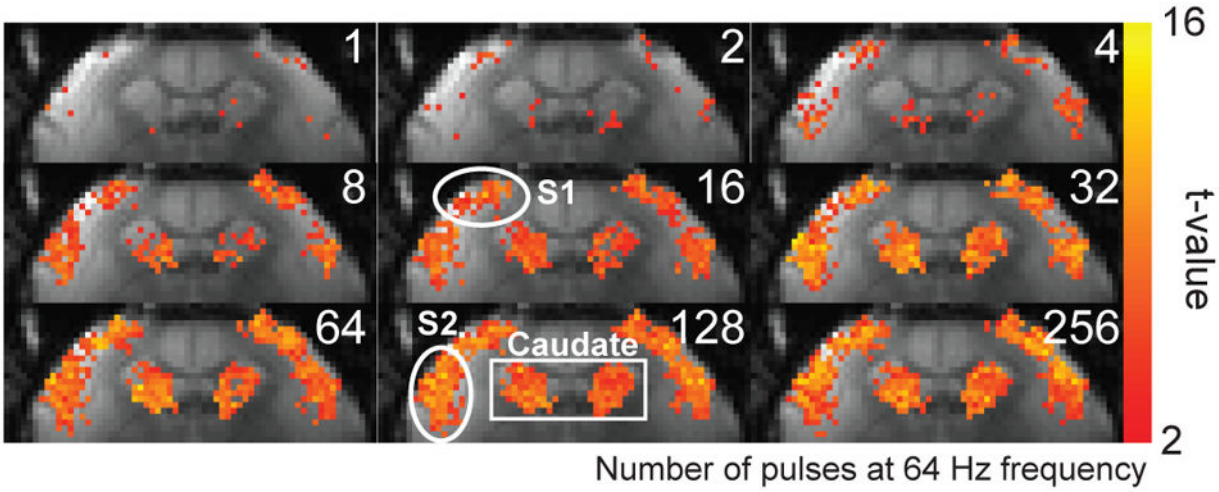

Figure 2.

(A) BOLD activation maps from a representative marmoset at different stimulus durations. Robust activation in response to bilateral somatosensory stimulation (2 mA amplitude, 333 μs pulses, 64 Hz) was observed in S1, S2 and caudate. The regions of activation in S1 and S2 grew with stimulus durations of up to 64 pulses (1 s). In caudate, the region of activation grew with stimulus durations of up to 32 pulses (0.5 s).

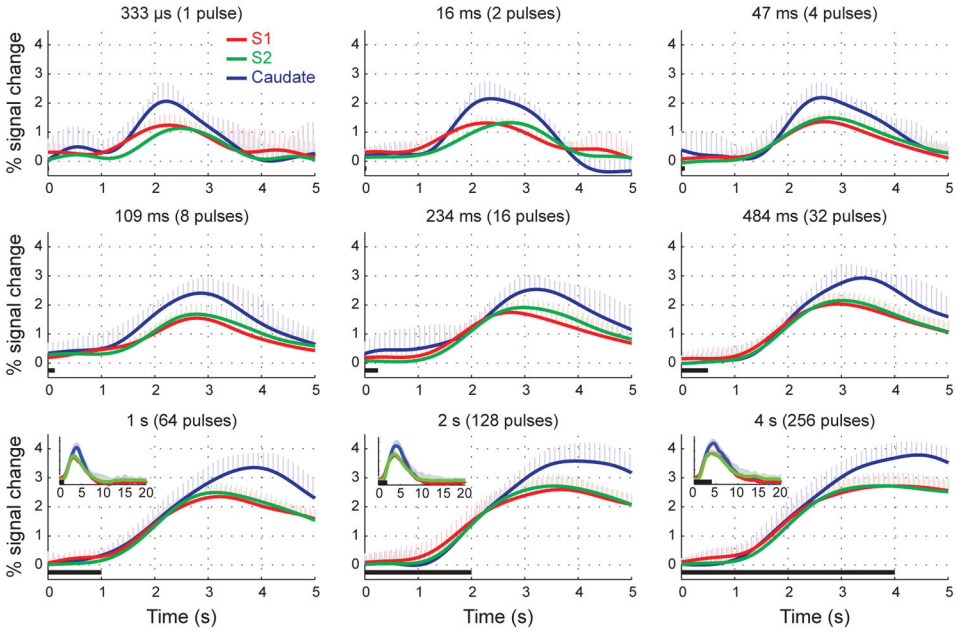

Figure 3.

Time-courses of the BOLD HRF to stimuli of increasing durations, averaged across subjects. Robust BOLD HRFs were obtained in S1, S2 and Caudate for all stimulus durations. The caudate region presented the strongest BOLD response, while S1 and S2 presented equivalent peak amplitudes. In all regions, the amplitude of the BOLD HRF grew with stimulus durations up to 1 s, and saturated in response to stimuli of longer durations. Error bars = 1 std. dev.

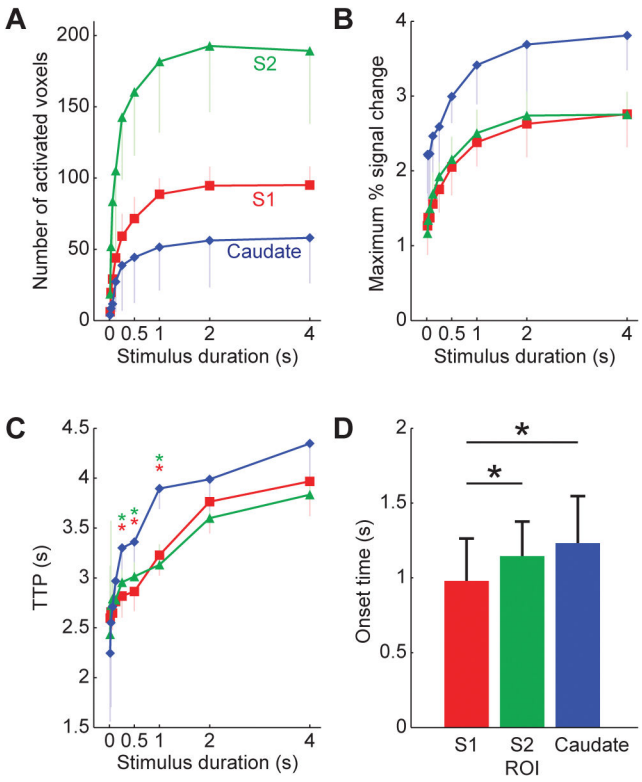

Figure 4.

(A) Plot of the mean growth in the size of the regions of activation in S1, S2, and caudate with stimulus duration, averaged across all five subjects. (B) Plot of the peak amplitude of the BOLD HRF in S1, S2, and caudate with stimulus duration, averaged across all five subjects. There was a monotonic increase of the number of active voxels and peak amplitude with stimulus durations up to 1s, and saturation for longer stimuli. (C) Plot of the time-to-peak (TTP) in S1, S2 and caudate with stimulus duration, averaged across subjects. The caudate region presented the highest BOLD amplitude and the longest TTPs at all stimulus durations. (D) The mean onset-time (OT) for each of the 3 regions, averaged across subjects. $^{*}P < 0.05$, one-way ANOVA followed by Scheffe post hoc test.

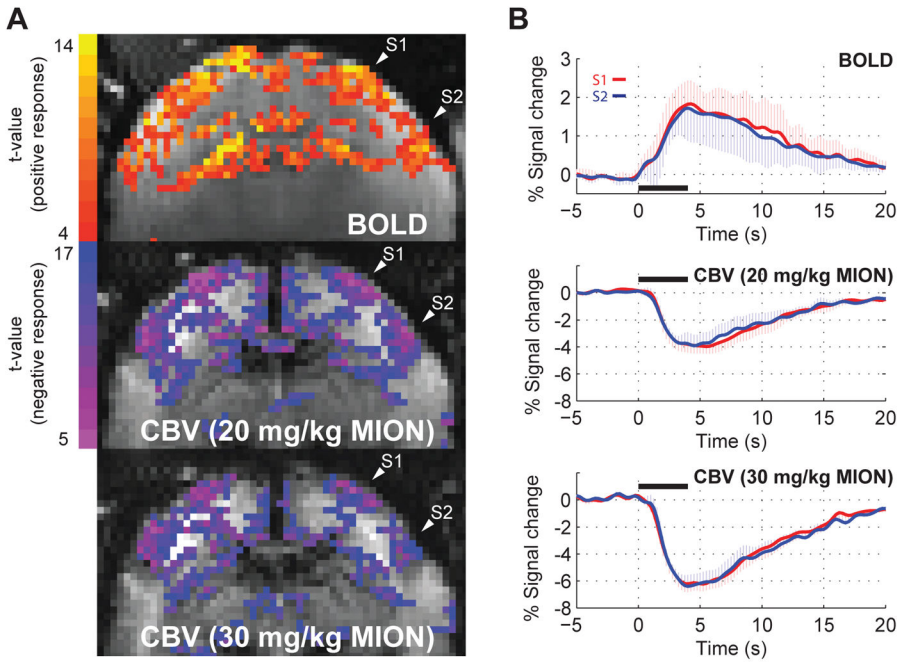

Figure 5.

(A) BOLD (top) and CBV t-score functional maps obtained at two different doses of MION (middle: 20 mg/kg; bottom: 30 mg/kg) in response to a 4 s stimulus duration. Robust BOLD and CBV activations were observed in S1, S2 and caudate. However, caudate showed no CBV activation at either dosage of MION. (B) Mean BOLD HRF (top graph) and mean CBV HRFs obtained with the lower dose (middle graph) and the higher dose of USPIO (bottom graph), in response to a 4 s stimulus, averaged across all five subjects. A stronger CBV response was observed at the higher dose of 30 mg/kg. Error bars = 1 std. dev. *P < 0.05.

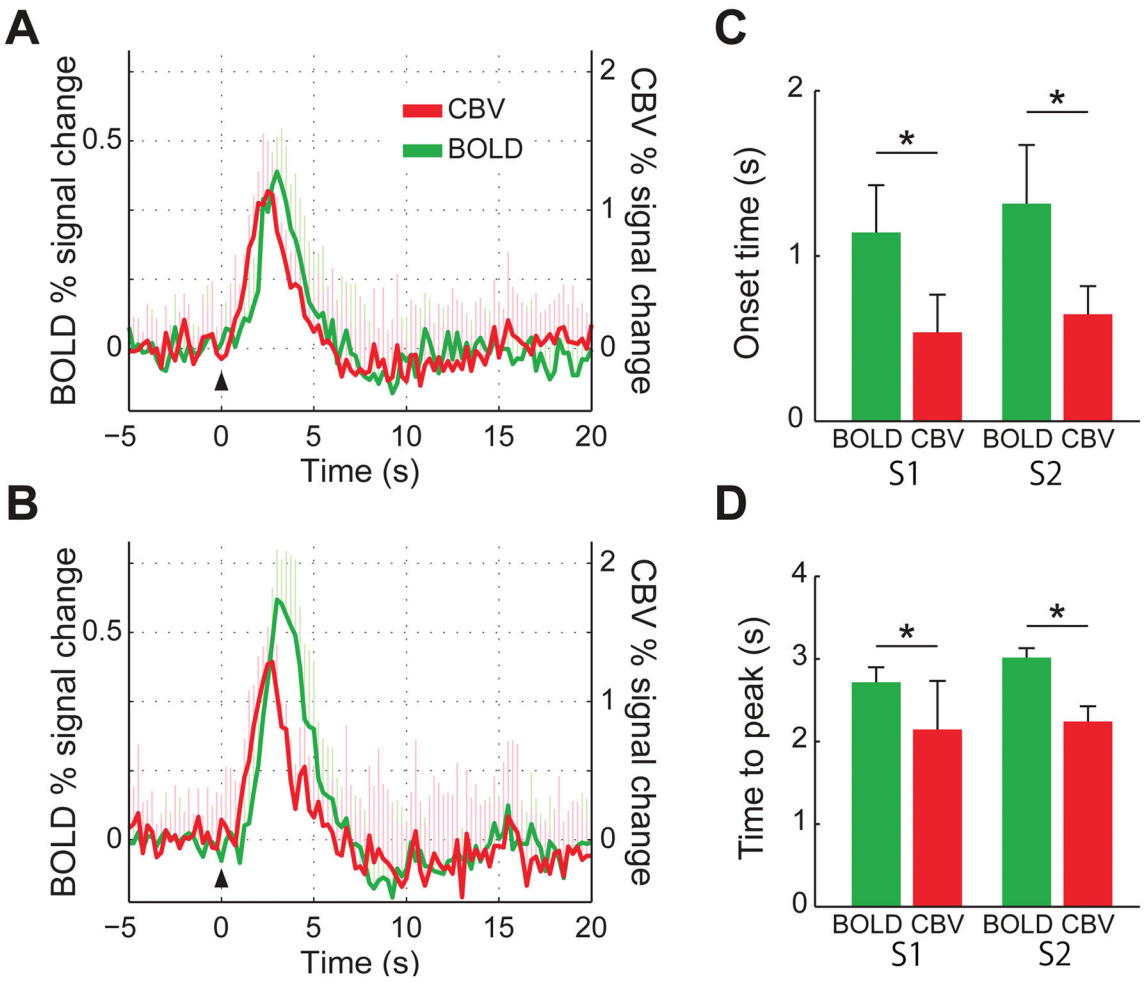

Figure 6.

(A) Mean BOLD (green) and CBV (red) HRF to a single 333 μs-long stimulus, measured in S1 and averaged across all five subjects. (B) Mean BOLD (green) and CBV (red) HRF to a single 333 μs-long stimulus, measured in S2 and averaged across all five subjects. (C) Mean onset times (OT) for BOLD (green) and CBV (red) in S1 and S2, averaged across all five subjects. (D) Mean times-to-peak (TTP) for BOLD (green) and CBV (red) in S1 and S2, averaged across all five subjects. In both regions, CBV had significantly shorter OT and TTP than BOLD. Error bars = 1 std. dev. *P < 0.05.

Table 1

Behavioral assessment scale.

Score	Behavior
1	Quiet: marmoset calm and relaxed
2	Mostly quiet, agitated only initially
3	Mostly quiet, with brief, intermittent mild agitation
4	Quiet after initial struggle, increasingly agitated over time
5	Mild agitation for about half of the restraint period
6	Moderate agitation during half of the restraint period
7	Restless and agitated during most of the restraint period
8	Extremely agitated during most of the restraint period

Table 2

Peak amplitude (% signal changes ± SD) of the BOLD HRF to different stimulus durations.

	1 pulse 333 μs	2 pulses 16 ms	4 pulses 47 ms	8 pulses 109 ms	16 pulses 234 ms	32 pulses 484 ms	64 pulses 1 s	128 pulses 2 s	256 pulses 4 s
S1	1.3±0.4*	1.4±0.2*	1.4±0.3*	1.6±0.2*	1.8±0.3*	2.1±0.4*	2.4±0.3*	2.6±0.5	2.8±0.4
S2	1.2±0.2*	1.3±0.1*	1.5±0.3*	1.7±0.4*	1.9±0.3*	2.2±0.3*	2.5±0.3*	2.7±0.4	2.8±0.3
Caudate	2.2±0.5*	2.2±0.6*	2.2±0.6*	2.5±0.5*	2.6±0.5*	3.0±0.4*	3.4±0.5	3.7±0.6	3.8±0.5

*Significantly different from the response to a 256 pulse stimulus ($P < 0.05$, one-way ANOVA followed by Dunnet post hoc test)